Performance of an Experimental 384 kb/s 1900 MHz OFDM Radio Link In a Wide-Area High-Mobility Environment

Bruce McNair, Leonard J. Cimini, Jr., and Nelson Sollenberger

AT&T Labs - Research,
100 Schulz Drive, Red Bank, New Jersey 07701-7033

e-mail: bmcnair, ljc, nelson@research.att.com

ABSTRACT

The first phase of an experimental investigation into future generation high-speed, high-mobility, wireless data communications techniques using OFDM has recently been completed. This paper reports on a prototype radio link intended to provide a high-speed downlink for wireless Internet access. Practical RF impairments and realistic algorithms have been studied to address the emerging need for data network access from high mobility platforms at wired LAN-like data rates.The performance of a prototype has been measured under a variety of radio channel conditions, including channels with two equal rays with from 2 to 20 μsec of delay separation and GSM channel models. Doppler fading rates from 1-200 Hz were tested. Measured results were compared with an idealized (e.g., no timing or frequency offset, no interchannel interference, etc.) simulation to verify the accuracy of the real-time implementation. Close agreement between the real-time prototype measurements, theory, and idealized simulations were observed.

1. INTRODUCTION

The interest in wireless high-speed access to wide area data networks has grown considerably in recent years. This growth is fuelled by the simultaneous development of the high-speed *wired* data networks (e.g., the Internet), significant improvement in data network access speeds (e.g., cable modems and DSL), wide-spread availability of powerful mobile computing devices (e.g., PDAs and notebook computers), rapidly dropping prices for increasingly sophisticated electronic devices, plus the global deployment of wireless voice systems. There is no reason to expect this momentum to decrease in the foreseeable future. For many users who are beginning to experience what high-speed global data access *or* untethered voice access can mean for them, the jump to wireless data access at near-LAN rates is attractive. Unfortunately, the harsh radio environment, with fading, dispersion, noise, limited spectrum, power restrictions, and a host of other constraints creates challenges when trying to provide this high-speed access, especially when the high-mobility seen in today's cellular networks is expected.

A related paper in the conference proceedings[4] describes the implementation of the experimental OFDM radio link presented in this paper. The reader is referred to that paper for a background on OFDM and the details of the radio link implementation. In this paper we briefly describe the OFDM radio link that was designed, define the experimental setup, and present performance results for a variety of channel conditions.

2. SYSTEM OVERVIEW

OFDM has been considered for use in high-speed wireless access networks[1][2] due to its robust performance on a dispersive channel. For the types of high-mobility, wide-area systems we have been considering, OFDM appears to provide an interesting alternative to other modulation techniques, especially where efficient implementation and flexible bandwidth assignments are considerations.

For the system under consideration, we chose to build a prototype 384 kb/s radio link that would provide robust performance in an 800 kHz RF bandwidth. With a tone spacing of 4.232 kHz, 189 tones can be accommodated in the chosen bandwidth. Using DQPSK modulation on each tone and a rate-½ Reed-Solomon channel code, a raw channel rate of 1.3104 Mb/s easily provided the desired 384 kb/s end user data rate.

The 189 QPSK modulated tones are transformed into 512 FFT samples. These samples are cyclically extended to tolerate with up to 20.3 μsec of delay spread. When combined with ramp and guard samples this results in OFDM block that is 288.461 μsec (625

samples at a 2.166 MHz sample rate) yielding 3.467 kbaud.

Additional details of the modulation and coding techniques and link parameters can be found in the associated paper[4].

3. EXPERIMENTAL MEASUREMENT SETUP

Figure 1 illustrates the setup that was used for performance measurements of the completed OFDM system. As seen in the figure, the DSP baseband transmitter generates I and Q samples, which are input to a pair of reconstruction low-pass filters. This filtered I and Q information is input to the RF unit, which translates the signals up to 1900 MHz. The transmitted RF signal is sent to a two-channel TAS-4500 RF channel fading simulator (fader), which simulates the response of two independent channels. The outputs of the fader are combined with independent noise signals, and the resulting faded signals plus noise are input to the two receiver RF branches and baseband processing. Fixed attenuators allow the signal levels and noise levels to be independently set for each branch. While performance measurements might be interesting for different signal-to-noise ratios on the two branches or for different signal levels (due to different antenna efficiencies), to reduce the number of test cases, all measurements were made with equal signal strengths and SNRs. We expect that a good receiver and antenna design would eliminate these variables. Likewise, it would have been possible to adjust the correlation between receiver branches, but for the purposes of these experiments, the correlation was set to zero. Other experiments[5][6] have shown that, for narrowband systems, the typical levels of antenna correlation experienced are low enough to create little degradation in antenna diversity performance. The tone-by-tone narrowband nature of the OFDM modulation will preserve the benefits of low correlation between antennas.

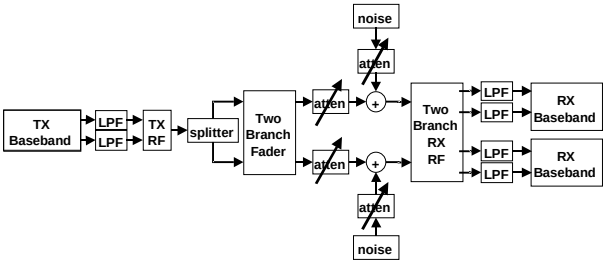

Figure 1 - Experimental Measurement Setup

To make the results of these experiments comparable to other results, it is necessary to define the method used to specify the SNR presented in the performance section below. Since it is generally difficult to separately measure signal power and noise power after they are combined in the receiver, it was necessary to separate them externally. With the arrangement shown in Figure 1, signal power and noise power could be independently controlled. Thus, by setting the noise attenuator to a very high level, e.g., 100 dB, essentially no excess noise was added to the signal. In the absence of noise, the signal level could be set to a reasonable operating level for the receiver. In this case, with a signal level on the order of –50 dBm, signal power in the receiver could easily be measured. Any receiver front-end noise was significantly lower in level. This fact was verified by attenuating both the noise and the signal and measuring the receiver power and by calculating the expected power level, knowing the bandwidth and noise figure of the receiver.

Noise power was similarly measured, with the signal appropriately attenuated. Combining these signal measurements and noise measurements, plus the level calibration of the attenuators, allowed very accurate control of the SNR seen by the demodulator

4. RESULTS

To get a full picture of a wireless system's performance, it is necessary to test it in a variety of channel conditions. However, as more variables are added to any test plan, the number of test cases is multiplied. To keep the test time to a manageable level, we chose a subset of interesting cases.

First, the effect of delay spread needed to be tested. While it was believed that delay spread would not have much impact on the OFDM link, this needed to be verified. For a two-ray equal-amplitude model, delays of 2, 5, 10 and 20 μsec were chosen. While it was expected that 2, 5, and 10 μsec should not tax the system's robustness to delay spread, 20 μsec was added to push the limits of the cyclic extension. With 44 samples of cyclic extension and a 461.5 nsec sample period, 20 μsec was the worse delay spread we could hope to counter. In addition, to allow comparison with other systems' performance, the GSM Typical Urban, Bad Urban, Hilly Terrain, and Mountainous Terrain models[7] were chosen, providing more representative delay spread profiles than the 2-ray cases. For comparison, flat fading as well as performance on an AWGN channel were also tested. All channel conditions were tested for one- and two-branch receivers.

Because the application of the OFDM modem was to be in high mobility environments, it was necessary to test the effect of fading rates on system performance. Fading rates of 1, 5, 40, 100 and 200 Hz were chosen,

both to compare to existing simulations and to reasonably model operational environments. Fading rates of 1 and 5 Hz modeled quasi-stationary or pedestrian applications. To model a range of city or suburban driving speeds, 40 and 100 Hz were used, while 200 Hz was intended to model highway speeds.

Since there was not enough time to test all 92 possible cases, the subset chosen was:

- AWGN
- flat fading at four fading rates
- 5 μsec equal ray fading at all fading rates
- 40 Hz with all channel models (i.e., all equal ray delays plus all GSM models)
- three extreme cases of equal ray and fading rate: 2 μsec/200 Hz, 20 μsec/1 Hz, and 20 μsec/200 Hz
- Mountainous Terrain at 40 and 200 Hz
- Hilly Terrain at 40, 100 and 200 Hz
- Typical and Bad Urban at 1, 40, 100, and 200 Hz

4.1. AWGN Channel

To allow comparison with theory, the performance of a one- and two-branch receiver in AWGN was first measured. Figure 2 shows the error rate for these measurements. It can be seen that the two-branch receiver provides about 2.5 dB performance gain over a one-branch receiver. The AWGN environment is not representative of what the modem might encounter on a wireless channel. However, this set of measurements provided an initial check on the modem performance – the error rate versus SNR curve's shape at high SNR showed that there were no serious implementation impairments which may have created an error floor. In addition, since the error rate curves followed their classic shape to very poor SNRs, the robustness of the timing recovery algorithm in noise that we expected was verified.

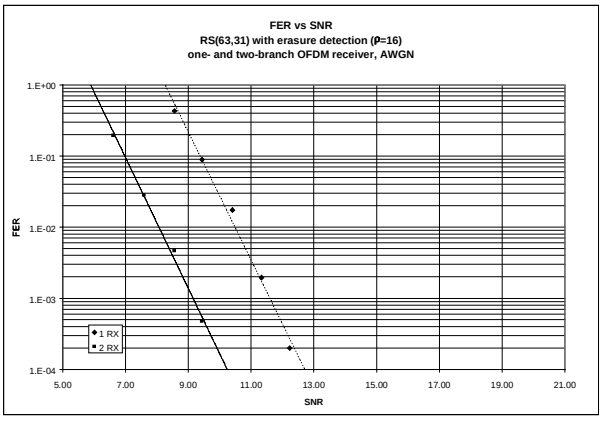

Figure 2 - Error rate for AWGN Channel

To compare receiver performance to theory, it is necessary to make a few conversions and simplifying assumptions. Applying simple combinatorics and assuming independence of Reed-Solomon symbol errors, the probability of correctly decoding a Reed-Solomon block, P_{CD}, for a code with codewords of length n, ν parity symbols used for correction, and a Reed-Solomon symbol error probability P_{CE} is. [8]:

$$P_{CD} = \sum_{i=0}^{\nu} \binom{n}{i} P_{CE}{}^{i} (1 - P_{CE})^{n-i} \tag{1}$$

Translating the Reed-Solomon symbol error probability into a QPSK symbol error probability requires that we consider that three QPSK modulated tones constitute one Reed-Solomon symbols. Therefore, assuming independence of the QPSK symbol errors, the relationship between the QPSK symbol error probability, P_Q, and the Reed-Solomon symbol error probability, P_{CE} is:

$$P_{CE} = 1 - (1 - P_Q)^3 \tag{2}$$

The symbol error probability P_m for differentially demodulated m-ary PSK, is related to channel E_b/N_0 as [9]:

$$P_m = 2Q\left\{\sin(\tfrac{\pi}{m})\sqrt{(E_b / N_0)\log_2(m)}\right\} \tag{3}$$

where

$$\begin{aligned} Q(x) &= \frac{1}{\sqrt{2\pi}}\left[\int_x^{\infty} e^{-\frac{t^2}{2}} dt\right] \\ &= \frac{1}{2}\left[1 - erf\left(\frac{x}{\sqrt{2}}\right)\right] \end{aligned} \tag{4}$$

Unfortunately, we know of no simple expression relating error rate to E_b/N_0 when some of the code's parity symbols may be marked as erasures. So, to bound the expected performance of the experimental system, we calculated the E_b/N_0 required for a (63,31) code with ν=16, that is, using all parity symbols for error correction, which should perform better than our system in AWGN. We then calculated E_b/N_0 required for a (47,31) code with ν=8, which has the error correcting capability of our system, but suffers from having no parity symbols available for dealing with erasures. In essence, the 16 erasure marking symbols of our (63,31) code may be viewed as being thrown away by the (47,31) decoder. Evaluating these equations for the two cases, we find that, in AWGN, to attain a 1% block error rate with a one-branch receiver, using differential QPSK modulation with the coding parameters as stated, the E_b/N_0 required is between 5.7 dB and 6.9 dB. E_b/N_0 is converted to SNR by adding 2.684 dB: +3.01 dB because 2 bits are transmitted per symbol, -.317 dB to account for the fact that the measured signal and noise power after the FFT do not

include non-FFT samples in the time domain waveform. Thus, we expect that the experimental one-branch OFDM modem should attain a 1% error rate between 8.4 and 9.6 dB SNR. Figure 2 shows that we attain this level of performance at 10.6 dB, which shows a good agreement with theory. Figure 3 shows the measurements for a single branch receiver, as well as the theoretical calculations that should bound the results. As shown, for error rates greater than 10^{-2}, the experimental results are within 1 dB of theory. As the SNR improves, theory predicts that the error rate will improve at an ever increasing rate. For the experimental system, implementation impairments (frequency offset, timing offset, intermodulation, interchannel interference, etc.) become larger with respect to the noise and the curves start to diverge slightly. Certainly, this will ultimately lead to an error floor in the measured data. However, we were not able to observe this floor in our experiments.

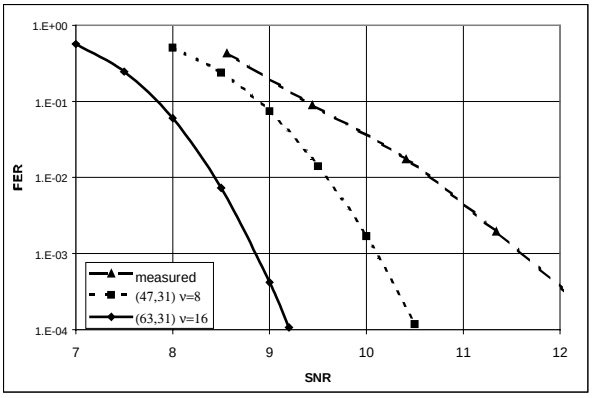

Figure 3 - Theoretical versus measured results, one-branch receiver, AWGN

4.2. Flat Fading

Beyond the noise in a simple AWGN channel, the next channel variable to be tested was fading. Although we expected that the true benefits of OFDM would best be seen in a dispersive channel, a flat fading channel was used to stress the system. Figure 4 illustrates the performance of one- and two-branch receivers at various fading rates. When compared Figure 2, it is immediately apparent how flat fading has degraded the receiver performance – at a 1% error rate, the receiver's performance has suffered at least 8 dB from the AWGN channel for a two-branch receiver. In addition, the slope of the curve in flat fading is much more shallow. Further, the performance measurements on a flat fading channel show that there is a relationship between error rate and fading rate, which will be discussed more fully below. Clearly, two-branch receiver diversity is much more effective in flat fading than it was on the AWGN channel, probably providing about an 8 dB advantage at 1% error rate, compared to 2.5 dB, but as will be seen later, channel coding is not able to realize its potential on the flat fading channel. As the channel fades, the SNRs at all frequencies are similarly degraded, so there is no opportunity to use "good" tones to compensate for the inevitable errors in the "bad" tones.

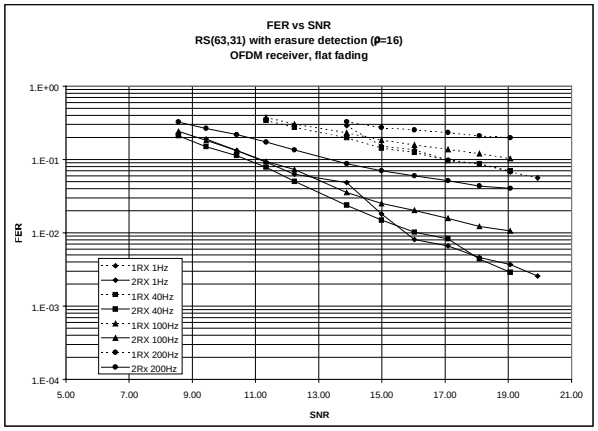

Figure 4 - Error rate for flat fading channels

4.3. Two-Ray Fading

Next, consider the performance of one or two receiver branches with 40 Hz fading and varying amounts of 2-ray equal-amplitude delay spread. Figure 5 illustrates the measured performance for these conditions. It can be seen that for moderate amounts of delay spread, up to 10 μsec, the performance of the OFDM receiver is essentially the same. When the delay spread gets to the limit of the cyclic extension, a small degradation in performance is evident – typically less than 1 dB. Further, since this figure depicts the performance with single and dual-branch receiver diversity, it can be seen that the diversity combining considerably improves receiver performance. At the target error rate of 1%, two-branch diversity has improved the receiver performance about 7 dB over the non-diversity case. Compared to flat fading, the improvement, mostly due to coding, is 4 dB for the two-branch case and considerably more for the one-branch case.

Figure 6 shows similar results, this time keeping the delay spread constant at 5 μsec while varying the fading rate. There are a few interesting features of these curves that are instructive to consider. First, the diversity improvement remains evident. Second, for low fading rates, there is little or no change in the error

rates of the receiver (1 Hz for the two-branch receiver is an exception that will be addressed later).

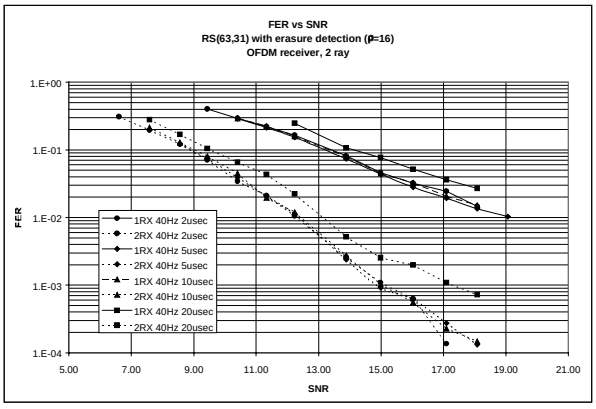

Figure 5 - Error rate for 2-ray channels at various delay spreads

As the fading rate increases to 100 Hz, less than 1 dB of performance degradation is evident for the two-branch diversity case and a little more degradation is evident for the single-branch case. What is quite evident is the severe degradation that occurs at 200 Hz fading rates. For the single-branch receiver, even at high SNRs, it is not possible to achieve even a 10% error rate, and for the dual-branch receiver, there is at least 4-5 dB of degradation at a 1% error rate. When we initially compared these results with prior simulations, it was quite surprising to see so much degradation in the receiver performance for 200 Hz fading rates. Below, we address the performance degradation in rapid fading.

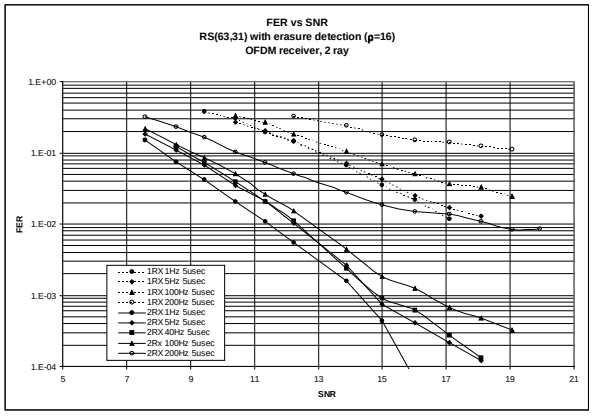

Figure 6 - Error rates for 2-ray channels at various fading rates

Returning to the 1 Hz, 5 μsec, two-branch case shown in Figure 6. It can be seen that the 5 Hz and 40 Hz curves are nearly identical, as they are for the single-branch case. However, in the single-branch case, the 1 Hz measurement was also nearly identical. Why does the two-branch receiver seem to perform about 1 dB better in 1 Hz fading? To understand this, we had to examine the behavior of the receiver on a fading, dispersive channel. As presented previously[3] our differential-in-frequency timing recovery algorithm attempts to track the centroid of the impulse response of the channel, which has the effect of minimizing the slope of the phase response of the channel plus receiver impairments. Because timing estimates made from individual blocks might be noisy, especially at poor SNR, averaging of the individual estimates was used. At the 1 Hz fading rate, one could observe the receiver timing following the individual fading rays. As the earlier ray on one channel increased in amplitude, the timing would adjust itself to follow that timing instant. As the later ray on the other channel increased in amplitude, the timing would move towards that timing instant. The result was that at the lowest fading rate, the timing always picked an optimal timing instant, rather than picking a midpoint in between the fading rays on the channel. In the one-branch receiver case, the higher effective noise level apparently masked the distinctively separate rays. This can be seen from the fact that the 1 Hz case begins to diverge from the higher fading rate cases at higher SNRs.

4.4. GSM Models

There is a set of standard delay profiles defined for GSM[7]. Figure 7 lists the amplitude and delay of each path in the two, five and six path models of these profiles. Some of the profiles have a component with moderate delay, e.g., 2 – 5 μsec, where an 800 kHz OFDM system should perform well. In addition, most of the models have a cluster of rays with relatively small delays, on the order of a few hundred nanoseconds. These smaller delays will tend to create a channel response that has flat fading-like qualities for the 800 kHz system.

Typical Urban		Bad Urban		Hilly Terrain		Mountainous Terrain	
Delay μsec	power	delay	power	delay	power	delay	power
0.0	.189	0.0	.164	0.0	.404	0.0	.909
0.2	.379	0.3	.293	0.2	.255	20.8	.091
0.5	.239	1.0	.147	0.4	.159		
1.6	.095	1.6	.094	0.6	.081		
2.3	.061	5.0	.185	15.0	.101		
5.0	.037	6.6	.117				

Figure 7 - GSM channel models

We tested the receiver performance with the GSM channel models described above. Figure 8 shows the

results for all of the GSM models with 40 Hz fading. As shown, for these channel models, the two-branch receiver performs 5-6 dB better than the one-branch receiver at a 1% error rate. The increased delay spread of the Bad Urban channel, which would heavily stress a single carrier equalized system, allows the OFDM receiver to deliver better performance than when operating on a Typical Urban channel, due to improved frequency diversity. On the other hand, Hilly Terrain and Mountainous Terrain perform more poorly than the urban models, since their long-delayed rays are significantly attenuated and do not substantially add to frequency diversity. We expect that, while the short delays between several rays of the Urban models create a flatter fading profile that limits the performance of our 800 kHz system, a wider bandwidth OFDM system should experience significant frequency diversity benefits even from the Typical Urban model.

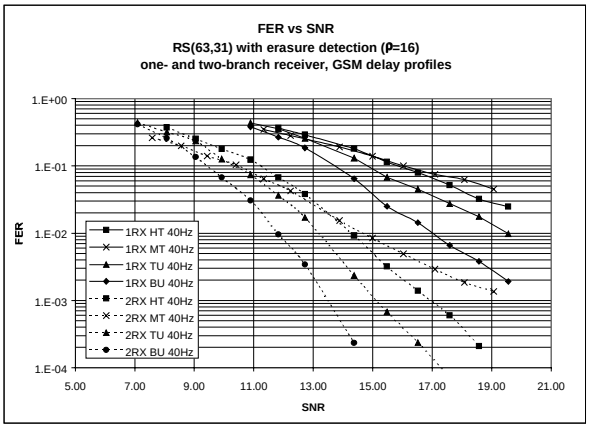

Figure 8 - Error Rates for GSM delay profiles at 40 Hz

The receiver performance was measured with several other fading rates. Since all cases demonstrated similar trends, only the Bad Urban and Hilly Terrain profiles are shown in Figure 8 for various fading rates. Bad Urban represents the best performance of the lot, Hilly Terrain represents nearly the worst. As seen previously, at moderate fading rates, for a given channel, the one- and two-branch receiver performance is consistent. However, as was the case for the two-ray channel, at 200 Hz, performance degradation of 1 dB or more is evident.

Figure 10 tabulates the results discussed above for a two-branch receiver. Here, we present the SNR required on various channels to deliver a 1% error rate. Blank entries in the table are for the measurements that were omitted from the testing. The "Bad Urban" case is so-called because of the relatively large RMS delay spread, which creates significant impairments for narrow-band, single-carrier systems. For the 800 kHz OFDM system, the larger delay spread creates very beneficial frequency selective fading. The Hilly

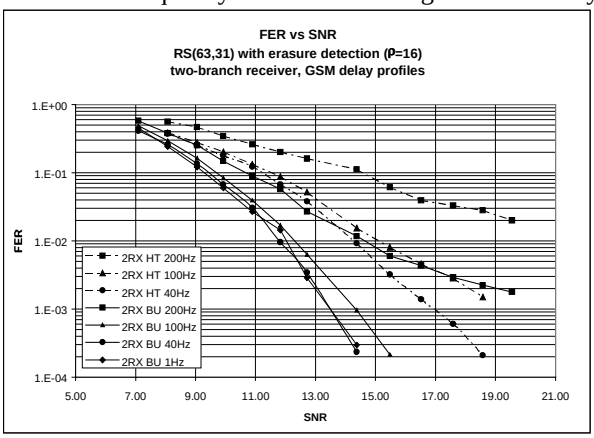

Figure 9 - Error Rates for GSM BU and HT at various fading rates

Terrain and Mountainous Terrain models, on the other hand, have larger amounts of delay spread, but do not distribute the transmitted energy as effectively. In both cases, the channel is modeled by one or more rays with relatively small delay spread plus a single ray that is 15 (HT) to 20 (MT) μsec delayed, but 10 dB below the less delayed signal(s). The effect of the single or closely spaced rays is to create a fading spectrum that often looks like flat fading. With a 10 dB reduction in the delayed ray, little variation from flat fading is created over the bandwidth of interest. Besides, as the two-ray measurements show, a delay of 20 μsec is stressing the limits of the cyclic extension.

Fading rate: Channel:	1 Hz	5 Hz	40 Hz	100 Hz	200 Hz	RMS Delay Spread
AWGN	8.0 dB					0.0 μsec
Bad Urban	12.0 dB		12.0 dB	12.2 dB	14.5 dB	2.4 μsec
2 μsec			12.2 dB		19.0 dB	1.0 μsec
5 μsec	11.4 dB	12.2 dB	12.2 dB	12.8 dB	18.3 dB	2.5 μsec
10μsec			12.2 dB			5.0 μsec
20μsec	12.2 dB		13.0 dB		>21 dB	10.0 μsec
TU	13.1 dB		13.3 dB	13.7 dB	16.5 dB	1.1 μsec
HT			14.0 dB	15.0 dB	~21 dB	4.5 μsec
MT			14.5 dB		>>21 dB	6.0 μsec
Flat	16.0 dB		16.0 dB	19.0 dB	>>21 dB	0.0 μsec

Figure 10 - SNR required for 1% error rate, two-branch receiver

Up to and including 100 Hz fading rates, it can be seen that the ordering of the performance by channel type is generally consistent. The exception (5 μsec/1 Hz) was discussed above where we found that the bandwidth of the timing recovery loop allowed the receiver to follow the channel from path to path. The unordered results for 200 Hz show that the relationship between performance and channel response is more complicated than would be explained by delay spread

alone. For the cases marked ">>21 dB," it was not obvious if the receiver performance would ever cross the target error rate, but if it did, the required SNR would be substantially more than 21 dB.

Figure 10 presents the results for the two-branch receiver only. Generally, with the one-branch receiver, a 1% error rate was only attainable at very high SNRs, if at all. In many cases, it was evident that an SNR of much greater than 21 dB would be needed or, in several cases, it was obvious that the receiver had reached an error floor above 1%. For this reason, Figure 11 summarizes the one-branch receiver performance but this time in terms of the SNR needed to attain a 10% error rate. Using the same ordering of the measurements from Figure 10, we see that the relative receiver performance for different channel conditions is similar to that for the two-branch case.

Fading rate: Channel:	1 Hz	5 Hz	40 Hz	100 Hz	200 Hz
AWGN	9.4 dB				
BU	13.4 dB		13.5 dB	14.4 dB	18.3 dB
2 μsec			13.5 dB		~21 dB
5 μsec	13.1 dB	13.1 dB	13.1 dB	14.0 dB	~21 dB
10 μsec			13.2 dB		
20 μsec	14.5 dB		14.0 dB		>21 dB
TU	14.4 dB		14.8 dB	15.5 dB	>21 dB
HT			15.8 dB	17.3 dB	>>21 dB
MT			16.0 dB		>>21 dB
Flat	17.1 dB		17.1 dB	19.1 dB	>21 dB

Figure 11 - SNR required for 10% error rate, one-branch receiver

Compared to the AWGN channel, for a one- or two-branch receiver, flat fading has degraded the SNR required to attain the target error rate by about 8 dB. For most of the delay spread channel conditions, the frequency selective nature of the fading allows the channel coder to mitigate about half of the degradation due to fading, or about 4 dB. While a 1% error rate was the target for the two-branch receiver, Figure 12

Fading rate: Channel:	1 Hz	5 Hz	40 Hz	100 Hz	200 Hz
AWGN	7.0 dB				
BU	9.3 dB		9.4 dB	9.7 dB	10.8 dB
2 μsec			8.9 dB		11.9 dB
5 μsec	8.1 dB	8.6 dB	8.9 dB	9.2 dB	10.4 dB
10μsec			9.1 dB		
20μsec	9.0 dB		9.5 dB		11.6 dB
TU	10.4 dB		10.5 dB	10.6 dB	12.0 dB
HT			11.2 dB	11.6 dB	14.2 dB
MT			10.4 dB		13.1 dB
Flat	11.2 dB		10.9 dB	11.2 dB	12.7 dB

Figure 12 - SNR required for 10% error rate, two-branch receiver

illustrates the SNR needed to attain a 10% error rate for the two-branch receiver, allowing a direct comparison with Figure 11. As the figure shows, two-branch diversity provided at least 4 and sometimes more than 8 dB performance advantage across the various channels.

4.5. Simulation Results

Figure 13 shows a comparison between the measured performance of the real-time OFDM modem and idealized simulations. The simulations do not include the effects of frequency or timing offset, nor do they model inter-channel interference. Since the simulations are performed in the frequency domain, they also exclude implementation details such as the cyclic extension. As we will describe below, while the frequency domain simulation captures most of the effects of channel coding, the effect of code word length on system performance is excluded. Thus, we expected that the simulations would demonstrate a somewhat optimistic performance.

We chose an two-ray equal-amplitude channel with 5 μsec of ray separation and 40 Hz fading rate as a baseline for comparison, using a rate-½ Reed-Solomon (63,31) code with ρ=16. As the figure shows, the difference between the simulation and the measured performance is .25 dB for error rates above .1%. The divergence at error rates below .1% is easily attributed to low level noise and distortion products. Given the implementation impairments that were expected and the idealized nature of the simulation, this was significantly better than expected.

We next compared the performance under higher delay spread conditions – this time 20 μsec of ray separation. As presented above, this amount of delay spread is at the limits of the cyclic extension. In the simulations, since there was no modeling of the time domain waveform, the higher delay spread simply moved the position of the nulls in the frequency response closer together, but did not change their character. Thus, the ~1 dB difference between simulation and measurements for this channel condition reflects the real time domain effects of high delay spread.

Next, we wanted to reconcile the difference between measurements and our expectations for high fading rates. As the figure shows, with a 5 μsec channel, from simulations we expect approximately a 2 dB degradation in performance at a 1% error rate. The measured results show a much higher level of degradation, about 6.5 dB. In fact, on a 200 Hz, 20 μsec channel, the receiver failed to achieve a 1% error rate and, based on the shape of the curve, this level of performance may not be not attainable at any SNR. Given the excellent agreement we had seen between

simulation and measurement and expectations from prior work, we wanted to better understand this problem.

Some prior simulations had used a (40,20) code, not the (63,31) code used here. We expected that, while the longer code word would have a greater probability of symbol errors, the stronger error and erasure correction properties of the longer code should prevail. On an AWGN channel, theory predicts that the longer code should perform about .4 dB better. Simulation showed that on the 5 μsec, 40 Hz channel, there was .25 - .5 dB degradation in performance for the shorter code. What was most notable about the results with the (40,20) code was performance at higher fading rates. With the shorter code, we did not see nearly the amount of degradation in system performance at higher fading rates that existed with the longer code. This gave us insight into the problems with the measured results at 200 Hz – with 288 μsec blocks, there was sufficient change in the channel response to begin to degrade the differential detection. In addition, since the simulation did not include time domain features, such as cyclic extension and guard time, the degradation in the differential detection was amplified.

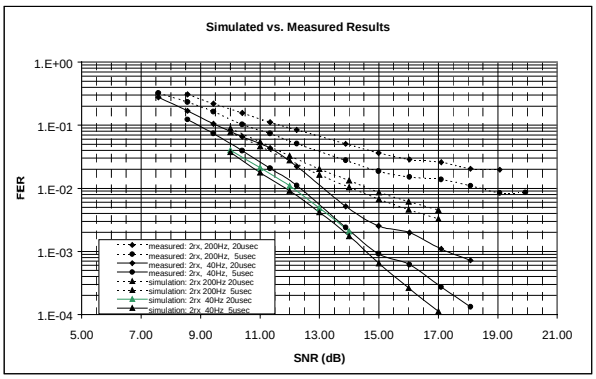

Figure 13 - Simulated and measured results for two-ray channel

5. CONCLUSIONS

We have described the performance of an OFDM modem intended for high-speed data access in wide-area, high-mobility applications. The modem performance has been demonstrated at the limits of the channel conditions that might be encountered in a cellular network, at high vehicle speeds. The experiments have demonstrated the practical considerations in OFDM system design and have yielded results that are being used to guide and validate decisions for the next generation, higher speed system.

Completion and testing of the 800 kHz OFDM modem also served to validate prior work on timing and frequency offset estimation. As evidenced by the measured performance at extremely poor SNRs and a wide variety of channel conditions, the synchronization algorithms demonstrated their robustness. Stable timing and frequency offset control were still evident even when OFDM blocks were being decoded with unusable error rates. The stability of these control functions was demonstrated by the small amounts of observable timing jitter and no apparent wander in frequency control, even when the demodulated constellation points were essentially lost in the noise.

The excellent agreement between measured performance and predictions based on theory and simulations gives us confidence that a practical, high-mobility OFDM radio link at near LAN-like rates is feasible. The value of frequency diversity through coding of the OFDM symbols within a block, as well as the improvement due to straightforward antenna diversity are evident from our experimental results.

REFERENCES

[1] L.J. Cimini and N.R. Sollenberger, "OFDM with Diversity and Coding for Advanced Cellular Internet Service," *Proceedings, IEEE Globecom'97*, pages 305-309, November 1997.

[2] J.Chuang, L.J.Cimini, G.Li, L.Lin, B.McNair, N.R.Sollenberger, M.Suzuki H.Zhao, , "High-speed wireless data access based on combining EDGE with wideband OFDM," ," *IEEE Comm. Magazine*, November 1999.

[3] B.McNair, L.J.Cimini, N.R.Sollenberger, "A Robust Timing and Frequency Offset Estimation Scheme for Orthogonal Frequency Division Multiplexing (OFDM) Systems," *Proc. VTC9*, pp.690-694, Houston, TX, May, 1999.

[4] B.McNair, L.J.Cimini, N.R.Sollenberger, "Implementation of an Experimental 384 kb/s Radio Link For High-Speed Internet Access," *Proc. VTC2000*, Boston, MA, September, 2000.

[5] B.McNair, "The Effectiveness of Preselection Diversity for Indoor Wireless Systems," *Proc. ICUPC97*, pp. 386-390, San Diego, CA, October, 1997.

[6] R.L.Cupo, J.Curlo, G.D.Golden, W.Kaminski, C.C.Martin, D.J.Mastriani, E.Rosenbergh, P.D.Sharpe, K.L.Sherman, N.R.Sollenberger, J.H.Winters, P.W.Wolniansky, and T.Zhuang, "Adaptive antenna applique field test," *Proc. Fourth Workshop on Smart Antennas in Wireless Mobile Communications*, Stanford University, July 1997.

[7] G.L.Stüber, *Principles of Mobile Communications*, pp. 84-86, Kluwer Academic Publishers, Boston, MA, 1996.

[8] A.M.Michelson, A.H.Levesque, *Error-Control Techniques for Digital Communications*, John Wiley & Sons, NY, NY, 1985.

[9] R.D.Gitlin, J.F.Hayes, S.B.Weinstein, *Data Communications Principles*, Plenum Press, NY, NY, 1992